

## Prediction of Paddy Straw Mechanical Properties under Varying Moisture Content and Loading Rate using ANN

Abhishek Patel<sup>1</sup>, Krishna Pratap Singh<sup>2\*</sup>, Ajay Kumar Roul<sup>1\*</sup>, Kamal Nayan Agrawal<sup>1</sup>, Karan Singh<sup>1</sup> & Manoj Kumar<sup>1</sup>

<sup>1</sup>ICAR-Central Institute of Agricultural Engineering, Bhopal 462 038, India

<sup>2</sup>ADG (Farm Engineering), ICAR-KAB-II, New Delhi 110 012, India

*Received 09 November 2022; revised 13 October 2023; accepted 29 December 2023*

In this work, the mechanical properties of paddy straw were evaluated using force-deformation curves and neural network approaches. The mechanical strength of the paddy straw was estimated at Moisture Contents (MC) of 10.8, 13.5, and 18.4% (w. b.), on distinguished internode positions, that is, N1, N2, and N3, and with applied Loading Rates (LR), that is, 25, 30, and 35 mm/min, respectively. Results shows that the values of Bending Strength (BS), Shear Strength (SS), and Young's Modulus (YM) were increasing from 5.35 to 17.34 MPa, 4.99 to 7.35 MPa, 0.43 to 1.39 GPa, respectively, through the node position from N3 to N1 with a decrease in MC and an increase in load through internode N1 to N3. Thus the MC and LR at different internode positions significantly ( $P < 0.05$ ) affected the BS, SS, and YM of paddy straw. The Levenberg-Marquardt's backpropagation based neural network was used to model the mechanical properties of paddy straw. The lower value of RMSE (0.69) and higher value of  $R^2$  (0.9998) indicates a best fit for the developed model. The coefficients of determination for BS, SS, and YM were 0.9994, 0.9942, and 0.998, respectively, indicating that the neural network model for estimating the mechanical properties of paddy straw can be used as an excellent alternative under selective experimental conditions.

**Keywords:** Bending strength, Force-deformation curve, Node positions, Shear strength, Young's modulus

### Introduction

Among cereal grains, paddy is one of the most essential and nutritional foods, consumed by more than 50% of the world population.<sup>1,2</sup> Annually, more than 800 million tons of paddy straw are produced in Asia and nearly 1 billion tons globally.<sup>3</sup> Only 1% of paddy straw is used by all the farmers.<sup>4</sup> More crop residues are left in the harvested paddy field because of the high straw grain ratio. Paddy straw is recognized as a significant agricultural by-product. It has variety of uses, including animal feed, useful organic input to farmlands, along with production of energy, briquettes, mushrooms, biogas, compost, and materials for packaging and biofuel for industries. The handling and processing of paddy straw are influenced by its physical, biological, and mechanical characteristics.<sup>2,5</sup>

The mechanical behavior of paddy straw must be considered during baling, transportation, and industrial processing. The improper chopping of paddy straw causes hair-pining phenomenon.

Therefore, to design a straw chopping machinery, the knowledge of engineering characteristics of paddy straw is imperative. The characteristics of the cellular straw material are influenced by the thickness of the straw, age of the crop, and cellular structure.<sup>6</sup> The mechanical characteristics of plants during their growth were focused in earlier investigations and noted that the paddy straw is delicate at low moisture content.<sup>7,8</sup> The physical and mechanical properties of straw changes due to the variation in plant growth and moisture content.<sup>9,10</sup>

The paddy stems were subjected to mechanical tests and the values of tensile strength, elastic modulus, and shear strength were 29.02 MPa, 1.03 GPa, and 8.52 MPa, respectively.<sup>11</sup> Another study investigated the strength parameters of wheat straw at different maturity stages and claimed that the average values of shear strength and YM ranged from 4.76 to 6.58 GPa and 4.91 to 7.26 MPa, respectively.<sup>12</sup> Similar results were observed in the alfalfa crop, where an increase in stalk moisture level resulted in a decrease in bending strength and increase in shear strength in the lower region of stem.<sup>9</sup> The values of SS, BS and YM for wheat straw were in the range of

\*Authors for Correspondence

E-mail: krishna.singh@icar.gov.in;\_ajaykroul@gmail.com

6.81–11.78 MPa, 6.81–11.78 MPa, and 0.65–1.82 GPa, respectively.<sup>13</sup> Other researchers reported the impact of moisture content, loading rate, and stalk cross section area on the shear and bending characteristics of barley straw.<sup>14</sup> Loading rate improved the SS of straw (paddy and wheat) for all the stem cross section areas.<sup>15</sup>

Numerous soft computing methods, such as neural networks, fuzzy-logic modelling, and other machine learning models were currently used for the analysis of physical and mechanical properties data of biological material. Artificial Neural Networks (ANN), is a supervised machine learning approach which mimics the function of a biological neuron. The ANN methodology can be used as a substitute for conventional realistic modelling depending on the regression.<sup>16</sup> There are no available literature on the prediction model using soft computing techniques for the effect of moisture content and loading rate on the mechanical properties of paddy straw. The aim of this study was to analyse the impact of moisture content and loading rate on the mechanical properties of paddy straw using an ANN model at different internode positions.

## Materials and Methods

### Experimental Study

The paddy (*c.v Kranti*) straw was procured from the Central Institute of Agricultural Engineering research farm in Bhopal, Madhya Pradesh (India) during the harvest season. The internodes were categorized into first, second, and third (N1, N2 and N3) group based on their placements below the ear (Fig. 1). In this study, the internodes N4 and N5, which represent the paddy stubble, are typically left in the field. Therefore, N4 and N5 were not used in this study. The complete leaf foliage and covering should be eliminated before the experimental study.<sup>7</sup> To evaluate the moisture content of paddy straw, the oven drying method was used. The samples were collected from the field on 0<sup>th</sup>, 5<sup>th</sup> and 10<sup>th</sup> day after harvesting.<sup>17</sup> Three different levels of moisture content of straw ( $10.8 \pm 1.2$ ,  $13.5 \pm 1.1$ , and  $18.4 \pm 1.4\%$  w.b.) and LR (25, 30 and 35 mm/min) were considered during the study.

### Mechanical Properties of Paddy Straw

#### Three-Point Bending Test

A three-point bending test was used to determine the maximum force to bend up to a certain

deformation. The length of the straw was 80 mm, and its two ends were rested on steel supports with contact arc lengths of 3 mm, as shown in Fig. 2. A Texture Profile Analyzer (TPA) (TA-XT Plus, Stable Micro Systems Ltd., Surrey, UK) was used to conduct the experiments using A/3PB probe. The TPA was set to the following parameters: pre-test speed: 1 mm/s; post-test speed: 3.33 mm/s; trigger force: 5 g; test speed: 0.42 mm/s; target mode distance: 15 mm; trigger type: auto and 200 Points Per Second (PPS) as data acquisition rate. The TPA analysis was carried out at room temperature (27 °C) and took 100 s for the process. Three different moisture content and load rates were used to examine the samples. Every specimen in the same lot underwent three measurements, and mean value was recorded.

Three loading rates (25, 30 and 35 mm/min) were used for the bending test to assess the force in the failure region of straw. By using the measured force, the YM and BS was computed. The straw was placed on two metallic supports that were rounded and spaced 80 mm apart, and a loading plate generated the load in the middle of the supports (Fig. 2b).<sup>10,13</sup> The straw samples were a little oval in cross-section and the second instant of area during the bending, denoted by the symbol  $I_b$ , explained as below.<sup>18</sup>



Fig. 1 — Representation of internode position of paddy straw

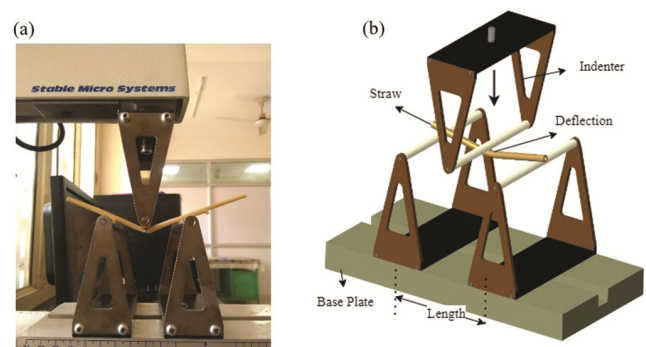


Fig. 2 — Three-point bending test rig: (a) Physical model on TMS-Prottexture analyzer and (b) CAD model of bending test rig

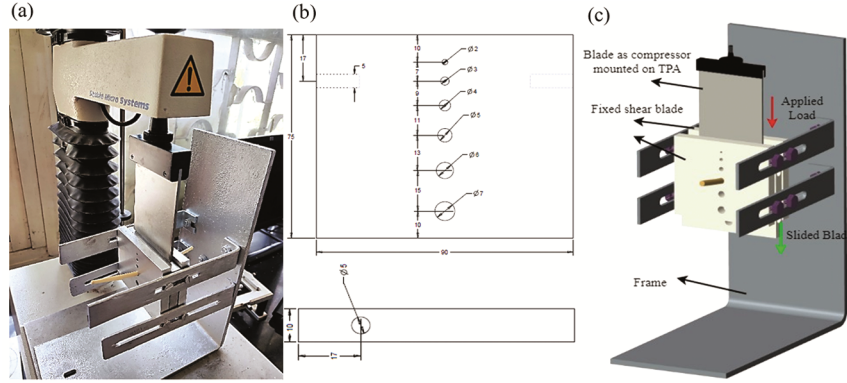


Fig. 3 — Shear strength measured by (a) shear plate test setup, (b) plate dimensions and (c) labelled cad model setup

$$I_b = \frac{\pi}{4} [ab^3 - (a-b)(b-t)^3] \quad \dots (1)$$

$$(BS) \sigma_b = \frac{\pi}{4} \left[ \frac{F_b a l}{4 I_b} \right] \quad \dots (2)$$

where,  $F_b$  = Bending force (N),  $I_b$  = Second moment of area ( $\text{mm}^4$ ),  $a$  = Semi-major axis (mm),  $b$  = Semi-minor axis (mm),  $\delta$  = Deflection length of straw (mm),  $l$  = Distance between supports (mm),  $t$  = thickness (mm), BS = bending strength (MPa)

#### Shearing Test

A force-time deformation graph was generated with respect to the experiment time, and shear force (SF) was determined with the help of above mentioned bending test procedure. The shear setup (Fig. 3) consists of three rectangular plates of aluminum material having holes of 2–7 mm diameter. The shear box was fabricated from an aluminum plate of overall dimensions  $90 \times 90 \times 25$  mm, having 5 mm thickness and 5 mm space between two plates.<sup>15</sup> The force was measured using an arrangement as said earlier and attached with a Warner Bratzler (HDP/BSW) probe to push the sliding plate of the shear plate setup.

$$(SS) \tau_s = \frac{F_s}{2A} \quad \dots (3)$$

where,  $F_s$  = Shear force at failure section (N),  $A$  = failure cross-section of the sample (mm).

To determine the shear strength of straw, similar results of shear tests were found, and the bending test was used to analyze the bending strength of straw.<sup>12,15,19</sup>

#### Young's Modulus

The given equation was used to evaluate the YM, and the process was similar to determining force, as stated earlier, for the determination of bending force.<sup>18</sup>

$$(YM) E = \frac{F_b l^3}{48 \delta I_b} \quad \dots (4)$$

where,  $E$  = Young's modulus (GPa)

#### ANN Modelling

ANN model was selected to forecast the mechanical characteristics of paddy straw using the MATLAB R2020a software. The input parameters, such as moisture content, internode position, and loading rate; output parameters, such as BS, SS, YM and one hidden layer were selected for the study. A backpropagation technique based on "Levenberg Marquardt" was used to set the weight and bias settings with neurons for optimization purposes.<sup>20,22</sup> To forecast the replies, a "tangent sigmoid" function was used as the hidden layer and a linear function as the output.<sup>20</sup> To find an appropriate model for fitting, the data set was split into training, validation, and testing. The hidden layer with varying numbers of neurons between 5 and 15 and the best network was determined by considering low Mean Square Error (MSE) and high coefficient of determination ( $R^2$ ) values. During the analysis of ANN, we followed the data with cross fold validation to estimate the performance of a model on the unseen data. It protects against overfitting of the predictive model. The model performance was assessed by accounting the chi-square ( $\chi^2$ ) value, mean absolute error (MAE) value, and root mean square error (RMSE) value. Low MAE, RMSE, and SE, as well as high  $R^2$  values, are characteristics of a well-trained ANN model.<sup>20,21</sup>

$$MAE = \frac{1}{n} \sum_{i=1}^n |P_i - E_i| \quad \dots (5)$$

$$RMSE = \sqrt{\frac{\sum_{i=1}^n (P_i - E_i)^2}{2}} \quad \dots (6)$$

$$\chi^2 = \frac{\sum_{i=1}^n (P_i - E_i)^2}{P_i} \dots (7)$$

where, the number of samples (n) is included in the dataset,  $E_i$  is the investigated value,  $P_i$  is the model predicted. The optimized network was assessed for each answer. The results were displayed alongside the actual data.

**Data Analysis**

The results were shown as the mean value and standard deviation of at least five replications. The treatment means were compared using all available variance-adjusted data (ANOVA), and Tukey's test determined that the variations were significant at the 95% level ( $p < 0.05$ ). In this work, Origin 8.0 software was used to produce the graphs, and SPSS Statistics 20.0 (SPSS Inc.) was used to analyze the data set.

**Results and Discussion**

The average values for the mechanical properties of paddy straw is presented in Table 1. There is a significant ( $p < 0.05$ ) effect of moisture content, loading rate and internode positions on the mechanical properties of straw.

**Impact of Moisture Content and Loading Rate on Bending Strength of Paddy Straw**

The interaction effect of moisture content and internode positions on the BS is shown in Fig. 4. The

bending strength is significantly ( $P < 0.05$ ) affected by the MC, LR and internode positions. The average values of BS at moisture contents, 10.8, 13.5 and 18.4%, were 11.97, 8.70 and 7.23MPa, respectively (Table 1). It was observed that, the bending strength decreased from 7.95 to 5.35, 10.79 to 6.24 and 17.34 to 10.09 MPa for N1, N2 and N3 (Fig. 4(a)) as the moisture content increased from 10.8 to 18.4%. Further, Fig. 4(b) depicts the interaction effect of the internode position and the LR on the bending strength of paddy straw. The mean values of the bending strength were 7.97, 9.49 and 10.45 MPa at loading rates 25, 30 and 35 mm/min, respectively (Table 1). It indicates a significant ( $P < 0.05$ ) drop in the bending strength from 7.81 to 5.59, 9.47 to 7.19 MPa and 14.04 to 11.28 MPa for N1, N2 and N3 with decrease in LR. The interaction effects between moisture content and internode (MC x NP); and loading rate (MC x LR) were significant ( $P < 0.05$ ), whereas the interaction effects of NP x LR was non-significant ( $P > 0.05$ ) on the bending strength.

**Impact of Moisture Content and Loading Rate on Shear Strength of Paddy Straw**

Based on the findings it could be said that the internode positions, moisture content, and loading rates significantly ( $P < 0.05$ ) affected the shear strength value of paddy straw. On the other hand, the shear strength was not affected significantly ( $P > 0.05$ ) by the

Table 1 — Impact of input parameters on the mechanical properties of paddy straw

Parameters	Levels	Bending strength (MPa)	Shear strength (MPa)	Young's modulus (GPa)
Moisture Content (%)	18.4	7.235 <sup>a</sup> ± 1.223	7.127 <sup>a</sup> ± 0.442	0.578 <sup>a</sup> ± 0.187
	13.5	8.707 <sup>b</sup> ± 2.123	7.498 <sup>b</sup> ± 0.032	0.696 <sup>b</sup> ± 0.169
	10.8	11.979 <sup>c</sup> ± 2.068	7.784 <sup>b</sup> ± 0.319	0.958 <sup>c</sup> ± 0.324
Loading rate (mm/min)	25	7.974 <sup>ab</sup> ± 1.235	7.138 <sup>ab</sup> ± 0.711	0.638 <sup>ab</sup> ± 0.135
	30	9.491 <sup>bc</sup> ± 3.442	7.313 <sup>ab</sup> ± 1.188	0.753 <sup>a</sup> ± 0.172
	35	10.457 <sup>ad</sup> ± 3.435	7.958 <sup>ac</sup> ± 0.779	0.832 <sup>b</sup> ± 0.274
Internode positions	N1	6.758 <sup>a</sup> ± 1.414	6.785 <sup>bc</sup> ± 0.195	0.541 <sup>ac</sup> ± 0.113
	N2	8.390 <sup>b</sup> ± 2.142	7.638 <sup>ac</sup> ± 1.236	0.670 <sup>b</sup> ± 0.171
	N3	12.773 <sup>c</sup> ± 3.494	7.986 <sup>ad</sup> ± 0.198	1.021 <sup>d</sup> ± 0.279

a-d: means with different letters are significantly different from others in the same line ( $P < 0.05$ )

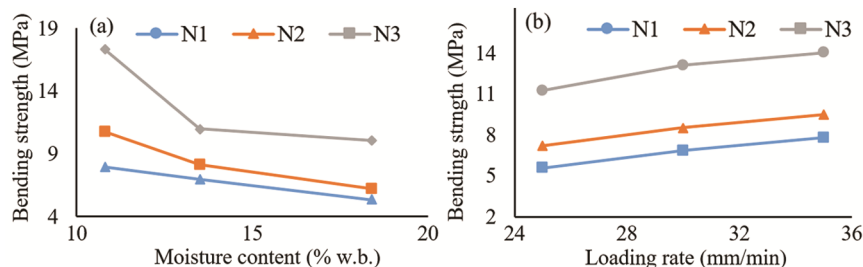


Fig. 4 — Impact of a) moisture content and b) loading rate on BS at different internode positions

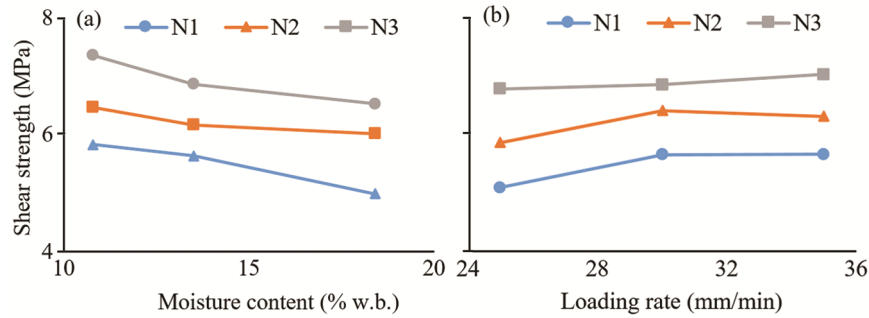


Fig. 5 — Impact of a) moisture content b) loading rate on shear strength at Various internode positions

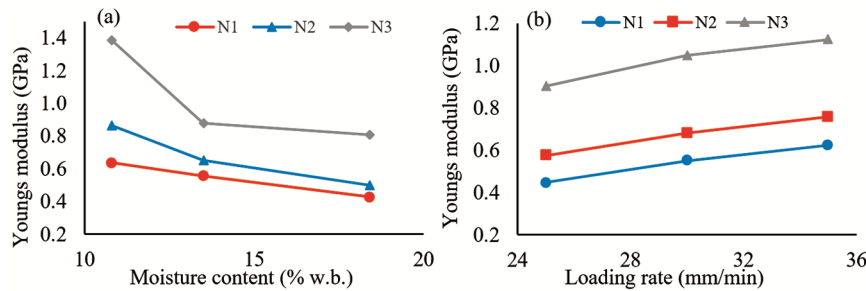


Fig. 6 — Impact of a) moisture content b) loading rate on Young's modulus at different internodes

interactions of MC × LR, MC × NP, NP × LR and MC × LR × NP. When the moisture contents varied from 18.4 to 10.8%, the average value of shear strength was between 7.127 and 7.784 MPa (Table 1). The interaction effect of the MC and internode position on BS is depicted in Fig. 5. With the increment in moisture content, the shear strength for the first, second, and third internodes reduced from 5.83 to 4.99, 6.47 to 6.01 MPa and 7.35 to 6.53 MPa (Fig. 5a). Whereas the interactional effect of internode position and loading rate on the bending strength is shown in Fig. 5b. The average shear strength at a loading rate of 25, 30, and 35 mm/min was 7.13, 7.31, and 7.96 MPa, respectively (Table 1). There is a significant ( $P < 0.05$ ) reduction in shear strength with the increase in loading rate was observed for the first, second, and third internode positions from 5.68 to 5.11, 6.33 to 5.88 MPa and 7.06 to 6.80 MPa, respectively.

**Impact of Moisture Content and Loading Rate on Young's Modulus of Paddy Straw**

The YM of paddy straw was observed to significantly ( $P < 0.05$ ) affected by the moisture content, rate of loading, and internode position. With the reduction in moisture content YM increased for all the internode positions. The interaction effect of the internode position and moisture content on the YM is shown in Fig. 6. Average values of YM with moisture contents of 10.8, 13.5, and 18.4% were 0.578, 0.696,

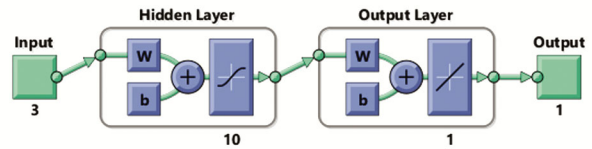


Fig. 7 — Multilayer feed-forward neural network architecture

and 0.958 GPa, respectively (Table 1). Young's modulus values for the N1, N2, and N3 declined from 0.64 to 0.43, 0.86 to 0.5 GPa and 1.39 to 0.81 GPa, respectively as the MC increased from 10.8 to 18.4%. (Fig. 6a). The mean values of YM were 0.63, 0.753 and 0.832 GPa, when the LR was increased from 25 to 35 mm/min (Table 1). It was noticed that the YM of the straw increased significantly ( $P < 0.05$ ) with the increase in LR for the first to third internode position (Fig. 6b). Young's modulus increases from 0.45 to 0.63, 0.58 to 0.76 GPa and 0.91 to 1.12 GPa for the internode position N1, N2 and N3, respectively with increasing load rate from 25 to 35 mm/min.

**ANN Model**

The neural network schematic topology is shown in Fig. 7. The total of hidden layers and neurons influence the accuracy of a neural network.<sup>20</sup> As shown in Table 2, the neurons with the lowest Mean Square Error (MSE) and high Correlation Coefficient (R) value for each response was chosen to create an ideal neural network. The low MSE values of the

Table 2 — MSE values of a neural network of predicted responses

Response	Hidden layer	No. of neurons	MSE		
			Training data	Testing data	Validation
BF	1	10	0.0049	0.0012	0.00015
SF	1	13	0.1582	0.0022	0.00009
YM	1	15	0.0076	0.0106	0.00026

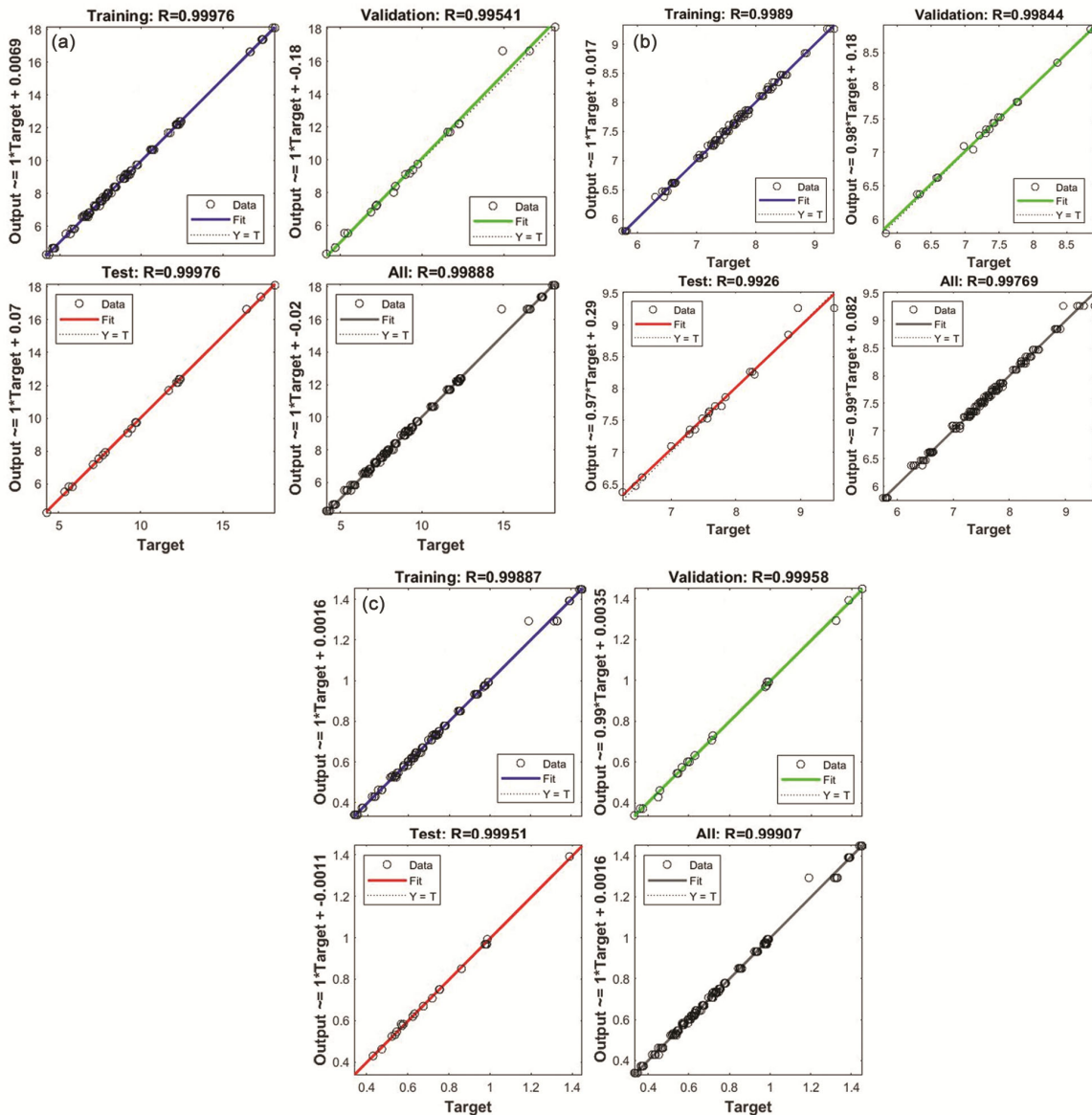


Fig. 8 — Regression analysis of model predictions of training, testing and validation data using ANN for (a) BS, (b) SS and (c) YM

training, testing and validation set indicate how close the data is to the actual data set with a better fit to the developed model.

From the regression analysis of the model plot (Fig. 8), it can be clear that the values used for the development of the ANN model predicted the data precisely with a high R-value for training, testing and

validation, respectively. The R value for training, testing and validation vary from 0.9926 to 0.9997, indicates the accuracy and best fit of the developed model.<sup>20</sup>

The statistical evaluation parameters of the developed ANN model are presented in Table 3. From the table, it can be seen that the MAE, RMSE, and  $\chi^2$

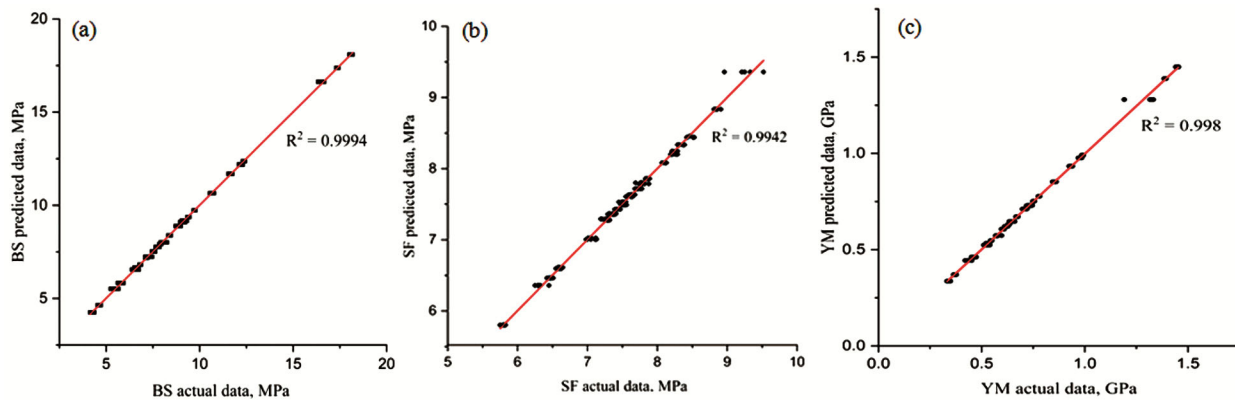


Fig. 9 — Experimental v/s predicted data of responses (a) BS, b) SS and (c) YM

Table 3 — Statistical evaluation parameters of the developed ANN model

Responses	MAE	RMSE	$\chi^2$	$R^2$
BS	0.0636	0.6996	0.1250	0.9994
SS	0.0396	0.4838	0.0570	0.9942
YM	0.0070	0.1053	0.0231	0.998

values vary from 0.0070 to 0.0636, 0.1053 to 0.6996, and 0.0231 to 0.1250, respectively. Similarly, the  $R^2$  value varies from 0.9942 to 0.9994 for all the three output parameters. The low value of MAE, RMSE,  $\chi^2$ , and high  $R^2$  value points the precise accuracy of the developed model over the experimental values. Similar results were found to evaluate the mechanical properties of canola stems using an artificial neural network.<sup>23</sup> The variation of investigational values with the model predicted values of mechanical properties such as BS, SS and YM is shown in Fig. 9. The  $R^2$  value of each response describes the goodness of fit of model with the investigational data. Indicators of data accuracy include a greater determination coefficient and lower data error. The nonlinear behaviour of the data set might explain the ANN model's improved ability to fit the data. When applied to the expected values, the constructed model performs well with some negligible residual errors, which may be due to the fact that the ANN model selects the data randomly.<sup>23</sup> Hence, the modelling of mechanical properties using an ANN gives a successful prediction of the output parameters of paddy straw.

## Conclusions

In the present study, an ANN model was developed to forecast the straw mechanical properties under various moisture content and loading rates. The outcome indicates that the shear strength was reduced with an increase in moisture content while it increased

with a surge in loading rate. As the loading rate increased toward the third internode, the bending strength and young's modulus also increased significantly. The mechanical properties of the paddy straw were strongly impacted by the input parameters, such as moisture content and loading rate. The developed ANN model can be used to envisage the bending strength, shear strength and young's modulus of paddy straw with the input parameters. The coefficient of determination values of experimental v/s predicted data for bending strength, shear strength and young's modulus were 0.9994, 0.9942 and 0.998, respectively. The ANN model developed in this research, can be used for the comparison of other machine-learning approaches in further studies. These results may be helpful for the design and development of crop harvesting machineries and industrial usage, respectively.

## Acknowledgements

The first author wishes to acknowledge the scholarship granted by ICAR-IARI for carrying out PhD research work.

## Conflict of interest

Authors declare there is no conflict of interest among them

## Funding:

This research received no specific grant from any funding agency in the public, commercial, or not-for-profit sectors.

## References:

- Zhang J, Li W, Zhou Y, Ding Y, Xu L, Jiang Y & Li G, Long-term straw incorporation increases paddy yield stability under high fertilization level conditions in the paddy-wheat system, *Crop J*, **9(5)** (2021) 1191–1197, <https://doi.org/10.1016/j.cj.2020.11.007>.

- 2 Patel A, Singh K P & Roul A K, Laboratory investigation on rotary impact cutter blade parameters for multistep cutting of paddy straw, *Indian J Ecol*, **50(2)** (2023) 519–525, <https://doi.org/10.55362/ije/2023/3929>.
- 3 McLaughlin O, Mawhood B, Jamieson C & Slade R, Paddy straw for bioenergy: The effectiveness of policymaking and implementation in Asia, in *24<sup>th</sup> European Biomass Conf Exhibit Amsterdam* (The Netherlands) (2016).
- 4 Patel A, Singh K P, Roul A K, Mahore A, Nalawade R D & Singh A K, Development and validation of an automatic recording microcontroller-based pendulum impact cutter, *Indian J Agric Sci*, **93(12)** (2023) 1356–1361, <https://doi.org/10.56093/ijas.v93i12.141548>.
- 5 Parihar D S, Narang M K, Dogra B, Prakash A & Mahadik A S, Rice residue burning in northern India: an assessment of environmental concerns and potential solutions – a review, *Environ Res Commun*, (2023), <https://doi.org/10.1088/2515-7620/acb6d4>.
- 6 Persson S, Mechanics of cutting plant material, An ASAE Monograph No. 7 *St. Joseph, MI, USA*, (1987).
- 7 Annoussamy M, Richard G, Recous S & Guerif, Change in mechanical properties of wheat straw due to decomposition and moisture, *Appl Eng Agric*, **16(6)** (2000) 657, [@2000](https://doi.org/10.13031/2013.5366).
- 8 Kushwaha R L, Vaishnav A S & Zoerb G C, Shear strength of wheat straw, *Can Agric Eng*, **25(2)** (1983) 163 – 166.
- 9 Galedar M N, Jafari A, Mohtasebi S S, Tabatabaefar A, Sharifi A, O'Dogherty M J & Richard G, Effects of moisture content and level in the crop on the engineering properties of alfalfa stems, *Biosyst Eng*, **101(2)** (2008) 199–208, <https://doi.org/10.1016/j.biosystemseng.2008.07.006>.
- 10 Tavakoli H, Mohtasebi S S & Jafari A, Effect of moisture content and loading rate on the shearing characteristics of barley straw by internode position, *Agric Eng Int*, **11** (2009) <https://cigrjournal.org/index.php/Ejournal/article/view/1176/1168>
- 11 Tang Z, Liang Y, Wang M, Zhang H & Wang X, Effect of mechanical properties of paddy stem and its fiber on the strength of straw rope, *Ind Crops Prod*, **180** (2022) 114729, <https://doi.org/10.1016/j.indcrop.2022.114729>.
- 12 O'dogherty M J, Huber J A, Dyson J & Marshall C J, A study of the physical and mechanical properties of wheat straw, *J Agric Eng Res*, **62(2)** (1995) 133–142, <https://doi.org/10.1006/jaer.1995.1072>.
- 13 Tavakoli H, Mohtasebi S S & Jafari A, Physical and mechanical properties of wheat straw as influenced by moisture content, *Int Agrophys*, **23(2)** (2009) 175–181.
- 14 Tavakoli M, Tavakoli H, Azizi M H & Haghayegh G H, Comparison of mechanical properties between two varieties of paddy straw, *Adv J Food Sci Technol*, **2(1)** (2010) 50–54.
- 15 Chandio F A, Changying J, Tagar A A, Mari I A & Guangzhao T, Comparison of mechanical properties of wheat and paddy straw influenced by loading rates, *Afr J Biotechnol*, **12(10)** (2013), <https://doi.org/10.5897/AJB12.2342>.
- 16 Behroozi K N, *Prediction of Dried Grape Quality by Artificial Neural Network*, MSc Thesis, Tarbiyat Moddars University, Bernacki, (2008).
- 17 ASAE Standards, Measurement–Forages. St. Joseph, MI, USA. (2006)
- 18 Gere J M & Timoshenko S P, *Mechanics of Materials*, 4<sup>th</sup> Ed (PWS Publishing Co, Boston) 1997.
- 19 Kumar A, Antil S K, Rani V, Antil P, Jangra D, Kumar R & Pruncu C I, Characterization on physical, mechanical, and morphological properties of Indian wheat crop, *Sustainability*, **12(5)** (2020) 2067, <https://doi.org/10.3390/su12052067>.
- 20 Selvan S S, Mohapatra D, Subeesh A, Kate A, Tripathi M K, Singh K & Kar A, Oxidation kinetics and an model for shelf life estimation of pearl millet (*Pennisetum glaucum* L.) grains during storage, *J Food Process Preserv*, (2022) e17218, <https://doi.org/10.1111/jfpp.17218>
- 21 Tripathy P P & Kumar S, Neural network approach for food temperature prediction during solar drying, *Int J Therm Sci*, **48** (2008) 1452–1459, <https://doi.org/10.1016/j.ijthermalsci.2008.11.014>
- 22 Kumar A, Srivastav P P, Pravitha M, Hasan M, Mangaraj S, Prithviraj V & Verma D K, Comparative study on the optimization and characterization of soybean aqueous extract based composite film using response surface methodology (RSM) and artificial neural network (ANN), *Food Packag Shelf Life*, **31** (2022) 100778, <https://doi.org/10.1016/j.fpsl.2021.100778>
- 23 Azadbakht M, Torshizi M V, Ziaratban A & Ghajarjazi, E, Application of artificial neural network (ANN) in predicting mechanical properties of canola stem under shear loading, *Agric Eng Int*, **18(2)** (2016) 413–425.